ELSEVIER

Thermochimica Acta 386 (2002) 27–34

thermochimica acta

www.elsevier.com/locate/tca

Thermodynamics of the NaX–DyX_3 (X = Cl, Br, I) molten salt systems

J.A. Baglio, L.R. Brock*, C.W. Struck

Osram Sylvania, Research and Development, 71 Cherry Hill Drive, Beverly, MA 01915, USA

Received 22 June 2001; received in revised form 21 August 2001; accepted 22 August 2001

Abstract

Rare earth metal halides in combination with alkali metal halides such as NaX–DyX_3 (X = Cl, Br, I) are used as part of the fill chemistry in high intensity discharge (HID) light sources. Thermodynamics descriptions of these metal halide melts are necessary to predict vapor compositions. While there are thermodynamic data available for the chloride and iodide based systems, there are no reported thermodynamic measurements and no published phase diagrams for the bromide system. Therefore, we have estimated the thermodynamic properties for the solid, liquid and gaseous NaBr–$DyBr_3$ system and calculated the gas phase concentrations of the various species present above melts with varying composition.

In order to accomplish this, we have relied upon the published phase diagrams of the NaCl–$DyCl_3$ and NaI–DyI_3 systems in addition to the reported enthalpies of mixing of the chloride system. Using a multi-species melt model (MSMM), we have found that we can get a reasonable phase diagram of the NaBr–$DyBr_3$ system together with reasonable enthalpies of mixing for all three systems. © 2002 Published by Elsevier Science B.V.

Keywords: Thermodynamics; NaCl–$DyCl_3$; NaBr–$DyBr_3$; NaI–DyI_3; Enthalpy of mixing; Phase diagram

1. Introduction

The intensity of the light emission and the color characteristics of high intensity discharge (HID) light sources are directly related to the alkali halides, metal trihalides and other additives within the arc tube of the light source. For this reason, it is important to know the composition of the vapor phase as a function of temperature and of the composition of the molten salt within the arc tube. Sodium and dysprosium halides are common HID arc tube additives. Therefore, we have used our multi-species melt model (MSMM), to calculate the thermodynamics properties of the NaX–DyX_3 (X = Cl, Br, I) molten salt systems. We then use this data to calculate the gas phase concentrations of the various species present above the melt within the arc tube.

While there are thermodynamic data available for the chloride and iodide based systems, there are no reported thermodynamic measurements and no published phase diagrams for the NaBr–$DyBr_3$ system. Therefore, we used the published phase diagrams for the NaCl–$DyCl_3$ [1,2] and NaI–DyI_3 [3,4] systems in order to bracket the NaBr–$DyBr_3$ system. Additionally, the known enthalpies of mixing of the NaCl–$DyCl_3$ [5–7] system were utilized to estimate the enthalpies of mixing of the NaI–DyI_3 and NaBr–$DyBr_3$ systems. These enthalpies of mixing were used in optimizing our estimates of the molten salts.

* Corresponding author. Tel.: +978-750-1534; fax: +978-750-1799.
E-mail address: Lori.Brock@Sylvania.com (L.R. Brock).

0040-6031/02/$ – see front matter © 2002 Published by Elsevier Science B.V.
PII: S0040-6031(01)00721-3

2. Free energy calculations

In order to describe the vapor species within an arc tube, thermodynamics descriptions of the vapor and of all condensed species including the multi-component molten salt are needed. To do this, we have solved a series of thermochemical equilibrium equations, namely the minimization of the free energy of the NaX–DyX_3 (X = Cl, Br, I) molten salt systems.

The free-energy minimization program, created by R.W. Liebermann for Osram Sylvania, minimizes the free-energy G,

$$G = \sum_i \mu_i n_i \tag{1}$$

under stoichiometric constraints. In Eq. (1), μ_i is the chemical potential, n_i the number of moles of the ith species and the sum runs over all species. In particular, the sum runs over all species in the gas phase, all single component condensed phases, and all species in every multi-component condensed phase.

The description of the multi-component gaseous system uses species which can be detected in mass spectrometric experiments. In addition, the thermodynamic quantities of the pure components such as NaI(l,s) and DyI_3(l,s) have also been measured. These simple liquids and solids are used to derive initial estimates of the thermodynamics of the condensed species. The species adopted to describe multi-component condensed liquids and solids need not and are not expected to have a detectible reality. This type of approach is not new, and has been used in the work of Hastie and Bonnell [8], where it is called the Associated Species Model, and also in the recent work of Spear et al. [9].

3. Phase diagram calculations

For the NaCl–$DyCl_3$ and NaI–DyI_3 systems, we considered known phase diagrams [1–4] to select the species needed in the MSMM and to create the thermodynamic descriptions of these species. For the NaCl–$DyCl_3$, the thermodynamics descriptions of the pure phases ($DyCl_3$(solid and liquid), NaCl(solid and liquid)) are combined to give initial descriptions of the multi-component melt species. These species are Na_3DyCl_6-(solid and liquid), $NaDy_3Cl_{10}$ (solid and liquid), $NaDyCl_4$(liquid), $NaDy_2Cl_7$(liquid), and $Na_7Dy_3Cl_{16}$-(liquid). For example, the enthalpy, entropy and heat capacity of $NaDy_2Cl_7$ associated liquid are given by Eqs. (2)–(4).

$$\Delta H_{f,298}(NaDy_2Cl_7) = \Delta H_{f,298}(NaCl(l)) + 2\,\Delta H_{f,298}(DyCl_3(l)) + \Delta_{298,H} \tag{2}$$

$$S_{298}(NaDy_2Cl_7) = S_{298}(NaCl(l)) + 2S_{298}(DyCl_3(l)) + \Delta_{298,S} \tag{3}$$

$$C_{p,T}(NaDy_2Cl_7) = C_{p,T}(NaCl(l)) + 2C_{p,T}(DyCl_3(l)) \tag{4}$$

The initial $\Delta_{298,H}$ and $\Delta_{298,S}$ are estimated, and then further refined to fit the phase diagrams [1,2]. Thermodynamic descriptions of the solids such as NaCl(s) and $DyCl_3$(s) are taken from the JANAF compilations [10] and our previous work [11]. Above the melt temperature, the solids are extrapolated smoothly so as to make the solids metastable. Above the melting temperature the NaCl(l) and $DyCl_3$(l) liquids are also taken from these sources. Below the melting point they were smoothly extrapolated to room temperature so as to make them metastable.

The accepted thermodynamic descriptions of the chloride system at 298 K are listed in Table 1. The accepted descriptions give the phase diagram shown as triangles and labeled ''calculated'' in Fig. 1. The two measured NaCl–$DyCl_3$ phase diagrams also appear in Fig. 1 [1,2]. The calculated phase diagram agrees well with the measured (literature) phase diagrams, typically falling between the two. The MSMM

Table 1
Thermodynamic quantities for the NaCl–$DyCl_3$ associated species

Condensed species	$C_{p,298}$ (J/mol K)	$S_{f,298}$ (J/mol K)	$\Delta H_{f,298}$ (kJ/mol)
$DyCl_3$(s)	95.04	155.23	−1008.34
$DyCl_3$(l)	90.86	187.61	−980.186
NaCl(s)	50.50	72.13	−411.12
NaCl(l)	49.66	99.08	−382.67
Na_3DyCl_6(s)	246.55	370.33	−2269.82
Na_3DyCl_6(l)	239.85	443.09	−2188.23
$NaDy_3Cl_{10}$(s)	335.63	535.55	−3447.62
$NaDy_3Cl_{10}$(l)	334.24	903.75	−2673.58
$NaDyCl_4$(l)	140.54	301.25	−1383.94
$NaDy_2Cl_7$(l)	231.38	527.18	−2352.37
$Na_7Dy_3Cl_{16}$(l)	620.24	1261.48	−5759.28

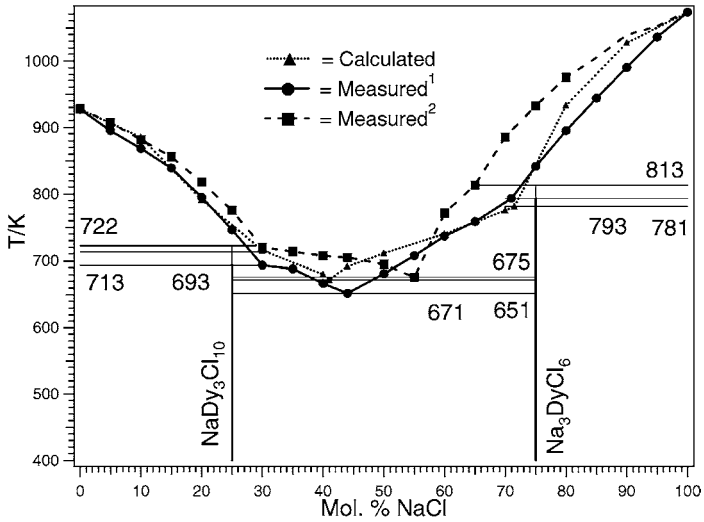

Fig. 1. A comparison of the two experimentally determined NaCl–$DyCl_3$ phase diagrams (shown as circles with a solid line and reproduced from Ref. [1], and squares with a dashed line reproduced from Ref. [2]) with the phase diagram calculated here using the MSMM (shown as triangles with a dotted line).

model predicts $NaDy_3Cl_{10}$ solid to decompose peritectoidally at 722 K, compared with 693 and 713 K of Refs. [1,2]. The MSMM predicts the eutectic at 781 K, compared with 793 and 813 K in Refs. [1,2]. The MSMM predicts Na_3DyCl_6 to decompose peritectoidally at 671 K, compared with 651 K at 71 mol% and 675 K at 65 mol% in Refs. [1,2]. We will postpone a more critical discussion of the extent of agreement between our predictions and the observed phase diagrams until we consider below the enthalpy of mixing that our description gives.

The NaI–DyI_3 phase diagram is calculated using the MSMM in the same manner as the chloride system. The phase diagram, shown in Fig. 2, has a simple eutectic at approximately 0.75 mol fraction NaI. The literature shows a halt in the phase diagram below the eutectic which is interpreted as the decomposition of some mixed iodide solid, taken as Na_3DyI_6(s), into

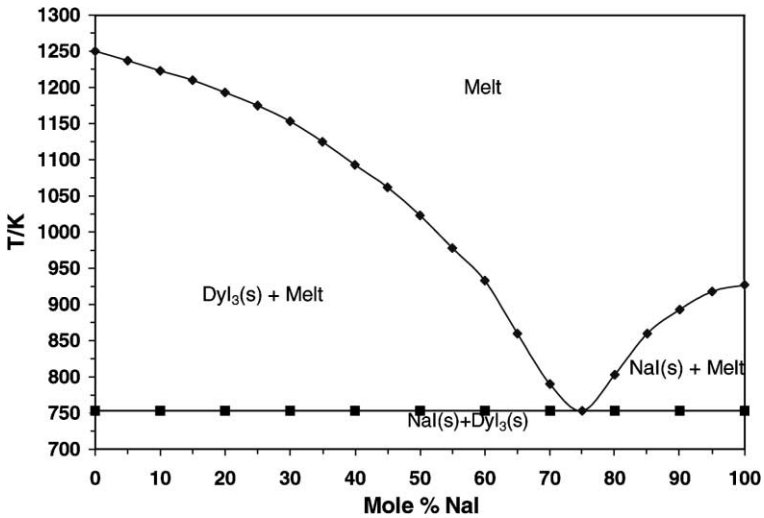

Fig. 2. The phase diagram of the NaI–DyI_3 system calculated using the MSMM showing a simple eutectic at approximately 0.75 mol fraction NaI.

Table 2
Thermodynamic quantities for the NaI–DyI_3 associated species

Condensed species	$C_{p,298}$ (J/mol K)	$S_{f,298}$ (J/mol K)	$\Delta H_{f,298}$ (kJ/mol)
DyI_3(s)	99.91	231.80	−596.22
DyI_3(l)	95.73	283.52	−535.13
NaI(s)	52.18	98.13	−289.53
NaI(l)	53.34	117.74	−270.71
Na_3DyI_6(s)	256.42	497.90	−1480.01
Na_3DyI_6(l)	255.74	586.46	−1405.2
Na_2DyI_5(l)	202.40	501.57	−1098.51
$NaDyI_4$(l)	148.99	377.36	−842.45
$NaDy_2I_7$(l)	244.79	646.31	−1359.8

Table 3
Thermodynamic quantities for the NaBr–$DyBr_3$ associated species

Condensed species	$C_{p,298}$ (J/mol K)	$S_{f,298}$ (J/mol K)	$\Delta H_{f,298}$ (kJ/mol)
$DyBr_3$(s)	98.81	196.65	−838.06
$DyBr_3$(l)	94.63	253.38	−775.60
NaBr(s)	51.40	86.82	−361.41
NaBr(l)	50.37	113.92	−334.36
Na_3DyBr_6(s)	252.99	456.06	−1933.01
Na_3DyBr_6(l)	245.73	585.76	−1828.41
$NaDy_3Br_{10}$(l)	334.24	903.75	−2673.58
$NaDyBr_4$(l)	144.99	382.84	−1129.68
$NaDy_2Br_7$(l)	239.62	635.97	−1895.98
$Na_3Dy_2Br_9$(l)	340.36	882.82	−2585.71
$Na_7Dy_3Br_{16}$(l)	636.45	1573.13	−4769.76

NaI(s) and DyI_3(s). We have not estimated the thermodynamic properties of this solid because it falls below the useful temperature range for HID lamp chemistry, and therefore we have not shown it in the figure. This phase diagram is reproduced with our description of six liquid species and three solid species.

The NaI–DyI_3 thermodynamic quantities for the associated species are given in Table 2. In order to check the validity of the phase diagram, we have compared the partial pressures of $NaDyI_4$(g) calculated from our description of the molten salt plus estimated thermodynamic descriptions of the $NaDyI_4$(g) over 0.5 NaI/0.5 DyI_3 liquid from Hildenbrand and Lau [12], and with Hilpert and Niemann's [13] published partial pressures measurements over 0.5 NaI/0.5 DyI_3 liquid. The experimental data is in good agreement with these calculations. The comparison is shown in detail in Ref. [4].

Once the thermodynamic quantities for the chloride and iodide systems were obtained, we were able to calculate the bromide system. The calculated NaBr–$DyBr_3$ phase diagram is shown in Fig. 3, and the thermodynamic quantities for the associated species are listed in Table 3.

In constructing the initial NaBr–$DyBr_3$ phase diagram, we assumed that its position lay between those of the chloride and iodide systems. It consists of a eutectic at ∼60 mol% NaBr at 722 K, and a compound Na_3DyBr_6 which decomposes peritectoidally at

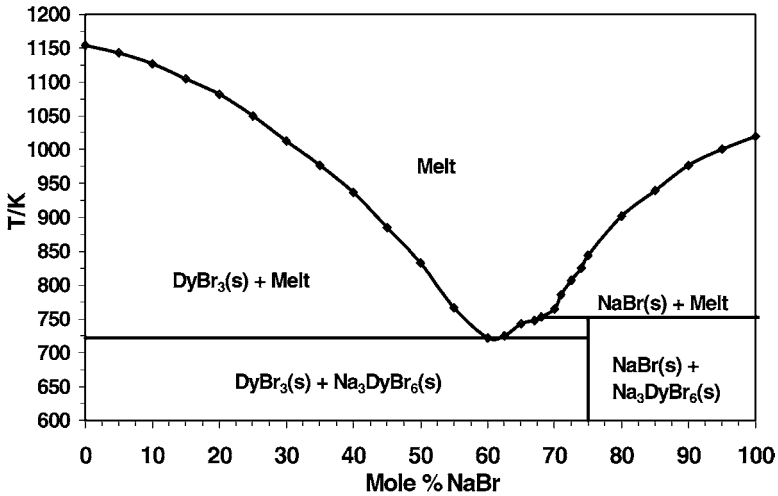

Fig. 3. The NaBr–$DyBr_3$ phase diagram calculated using the MSMM.

753 K. A total of six associated liquids (Na_3DyBr_6, $NaDy_3Br_{10}$, $NaDyBr_4$(l), $NaDy_2Br_7$, $Na_3Dy_2Br_9$, $Na_7Dy_3Br_{16}$), and one solid (Na_3DyBr_6) were used to calculated the phase diagram. Fine adjustments to the phase diagram were made to ensure that the heats of mixing of all three systems showed reasonable trends, as discussed below.

4. Heats of mixing

The heat of mixing, $\Delta H_{\mathrm{mix},T}(y)$, of a particular $y\mathrm{DyX_3} + (1-y)\mathrm{NaX}$ composition (where y is the mole fraction of $\mathrm{DyX_3}$) at 1100 K is the reaction enthalpy of the following reaction:

$$y\mathrm{NaX(l)} + (1-y)\mathrm{DyX_3(l)} = \mathrm{Na}_y\mathrm{Dy}_{(1-y)}\mathrm{X}_{(3-2y)} \quad (5)$$

The enthalpy of the ideal liquid is the mole fraction of each component multiplied by the enthalpy of that pure component

$$H_{1100\,\mathrm{K,ideal}}(y) = yH_{1100\,\mathrm{K,NaXl}} + (1-y)H_{1100\,\mathrm{K,DyX_3l}} \quad (6)$$

The enthalpy of the real liquid at a temperature T is the sum of the enthalpies of each associated species multiplied by its mole fraction.

$$H_{1100\,\mathrm{K,real}}(y) = \left(\sum_i f_i H_{\mathrm{f},1100\,\mathrm{K},i}\right) \quad (7)$$

where f_i is the mole fraction of the ith associated species at 1100 K for the composition $y\mathrm{DyX_3} + (1-y)\mathrm{NaX(l)}$.

The heat of mixing is the enthalpy of the real liquid minus the enthalpy of the ideal liquid.

$$\Delta H_{\mathrm{mix},1100\,\mathrm{K}}(y) = \left(\sum_i f_i H_{\mathrm{f},1100\,\mathrm{K},i}\right) - yH_{1100\,\mathrm{K,NaXl}} - (1-y)H_{1100\,\mathrm{K,DyX_3l}} \quad (8)$$

Fig. 4 shows a plot of the enthalpy of mixing, $\Delta H_{\mathrm{mix},1100\ \mathrm{K}}(y)$, of the NaCl–$DyCl_3$ system at 1100 K vs. the mole fraction of $DyCl_3$. The ΔH_{mix} values calculated using the MSMM are represented by triangles, and the experimentally obtained values are represented using open circles. The measured values were taken from the work of Gaune-Escard and co-workers [5–7] and fit to a fifth-order polynomial (shown as a solid line). The calculated values were similarly fit to a fifth-order polynomial, and the fit is shown as a dashed line through the triangles. The measured and calculated values are in good agreement, with the calculated values more negative in the 0.2–0.6 mol fraction

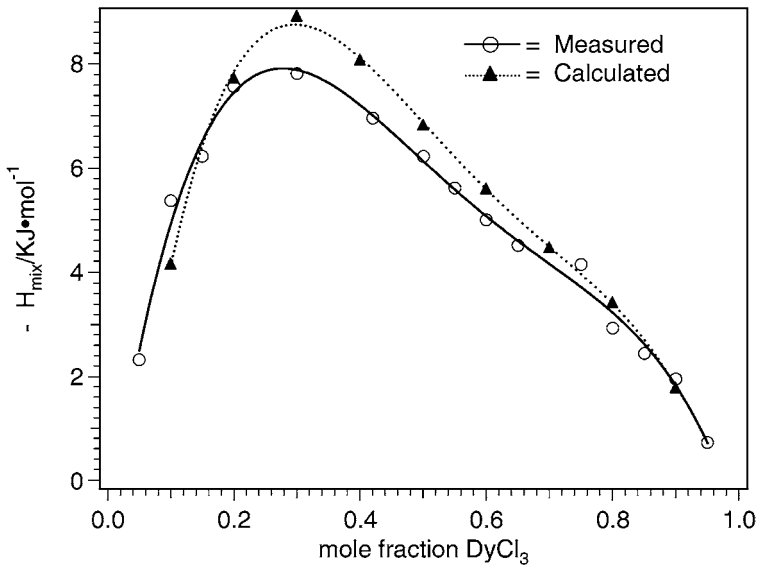

Fig. 4. A plot of the calculated (triangles with dashed line) vs. measured (circles with solid line) enthalpies of mixing ($-\Delta H_{\mathrm{mix}}$, kJ/mol) for the $DyCl_3$–NaCl melt at 1100 K. The measured data is taken from the work of Gaune-Escard and co-workers [5–7].

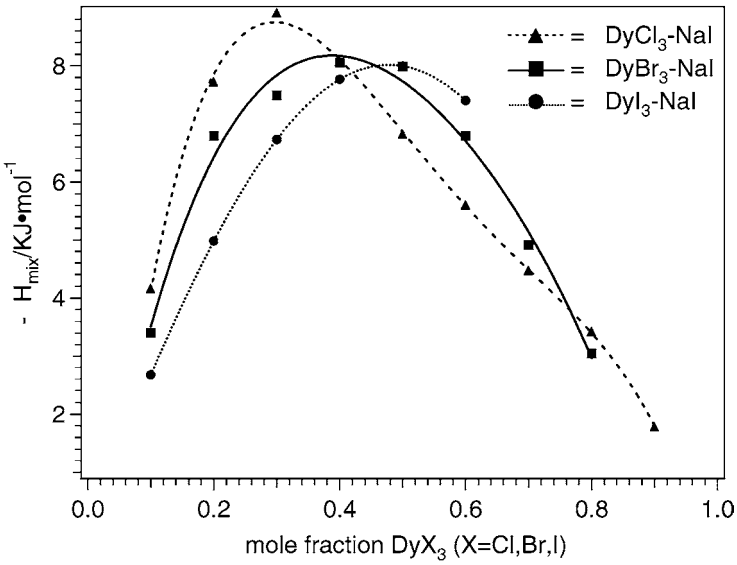

Fig. 5. A plot of the enthalpies of mixing ($-\Delta H_{\mathrm{mix}}$, kJ/mol) for the DyX_3–NaX (X = Cl, Br, I) melts at 1100 K. The enthalpies of mixing were calculated using the MSMM.

region. Additionally, both the measured and calculated ΔH_{mix} values exhibit a peak around 0.3 mol fraction.

Attempts to vary the calculated chloride system phase diagram to match more closely either of the two reported phase diagrams resulted in enthalpies of mixing that were much higher than the measured values.

Fig. 5 compares the enthalpies of mixing for the chloride, bromide and iodide systems. The results show reasonable trends among these three systems with the chloride giving the highest heat of mixing −8.91 kJ/mol near 0.3 mol fraction of $DyCl_3$. The heat of mixing for the bromide is −8.05 kJ/mol near 0.4 mol fraction of $DyBr_3$, while the maximum for the iodide is −8.00 near 0.5 mol fraction of DyI_3.

5. Entropy of mixing

The equation for the excess entropy of mixing is

$$\begin{aligned}\Delta_{\mathrm{xs}}S_{\mathrm{mix,1100\,K}}(y) &= \left(\sum_i f_i S_{\mathrm{f,1100\,K},i} - Rf_i \ln f_i\right) \\ &- (yS_{\mathrm{1100\,K,NaXl}} - Rx\ln(y)) \\ &- ((1-y)S_{\mathrm{1100\,K,DyX_3l}} - R(1-y)\ln(1-y))\end{aligned} \tag{9}$$

In Eq. (9), the first term on the first line is the entropy of the real solution. The second and third lines are the entropy of the ideal solution. The entropy of an ideal solution has in it the term for the entropy of mixing of an ideal solution, namely,

$$\Delta S_{\mathrm{mix,1100\,K}}(y) = -R(f_{\mathrm{l}}\ln f_{\mathrm{l}} + (1-f_{\mathrm{f}})\ln(1-f_{\mathrm{l}})) \tag{10}$$

We expect the entropy of mixing to be close to zero and negative. The entropy of mixing in the iodide case was found to be slightly negative (between 0 and −1). However, in the chloride and bromide cases, we calculate $\Delta S_{\mathrm{mix,1100\,K}}$ on the order of 0.5–10 J/mol K. No information regarding ΔS_{mix} for these melts is reported in the literature. We do accept the positive entropies of mixing where we expect slightly negative entropies of mixing as pointing to inadequacies in our model. However, we are not aware that any current model gives better predictions of this entropy of mixing.

6. Vapor phase

The phase diagram for the bromide system allowed for the calculation of the gas phase species concentrations over the melts that could be found in HID arc

Table 4
A comparison of the species number densities and ratios using the ideal solution model and the MSMM for the NaBr–$DyBr_3$ system[a]

Vapor species	Part/cm^3 (ideal solution)	Part/cm^3 (associated species)	Ideal solution/ associated species
Na_3Br_3	1.53E + 10	1.84E + 08	83.5
Na_2Br_2	1.30E + 15	6.81E + 13	19.1
$NaDyBr_4$	1.20E + 16	5.88E + 14	20.4
NaBr	4.81E + 15	1.10E + 15	4.4
Dy_2Br_6	7.20E + 13	3.31E + 12	21.7
$DyBr_3$	1.78E + 15	3.82E + 14	4.7
Total Dy	1.39E + 16	9.77E + 14	14.2
Total Na	1.94E + 16	1.82E + 15	10.6
Total Br	6.11E + 16	4.76E + 15	12.8
Na/Dy	1.39E + 00	1.87E + 00	

[a] Melt temperature 1100 K, volume 0.02272, Ar number density 6.64×10^{18}.

tubes. In order to determine if an MSMM was necessary to obtain reasonable vapor species number densities in HID lamp calculations, we compared our MSMM output to results obtained using only an ideal solution of NaBr(l) with $DyBr_3$(l). The results are shown in Table 4.

We have found that, even when reliable thermodynamic descriptions of the vapor are available, attempts to describe the molten salts of the NaBr–$DyBr_3$ system using only an ideal solution of NaBr(l) with $DyBr_3$(l) yields vapor Na and Dy species concentrations that are too high by factors ranging from 3 to 30. For example, in the case of a NaBr–$DyBr_3$ melt at 1100 K with molar ratios of 1:1, the ideal solution model gives the $NaDyBr_4$(g) number density a factor of 20 higher and the NaBr(g) number density a factor of 4.4 higher than that obtained with the more reliable MSMM.

The exact calculated values in Table 4 use private descriptions of the vapor species developed by our critical review of literature, by information obtained under contract from SRI, and from our estimating procedures [13].

7. Conclusions

We have used our MSMM to calculate the phase diagrams of the NaX–DyX_3 (X = Cl, Br, I) molten salt systems. The calculated chloride and iodide system phase diagrams were in good agreement with the measured phase diagrams found in the literature. No measured phase diagram was available for the bromide system, and therefore the thermodynamic quantities of the iodide and chloride systems were used to bracket the bromide system.

The enthalpies of mixing for all three molten salt systems were also calculated, and reasonable trends were obtained with the chloride having the highest $\Delta H_{\mathrm{mix,1100\ K}}$ followed by the bromide and then the iodide. The thermodynamic quantities obtained for the bromide system were used to calculate the gas phase concentrations of the various species present above a typical bromide melt that may be found within an HID lamp arc tube. As expected, attempts to describe molten salt systems of the NaX–DyX_3 type using only an ideal solution of NaX(l) with DyX_3(l) yields vapor Na and Dy species concentrations that are too high by factors ranging from 3 to 30. The multi-species melt model yielded more accurate results.

References

[1] B.G. Korshunov, D.V. Drobot, Zh. Neorgan. Khim. 10 (1965) 939.
[2] J. Mochinaga, H. Ohtani, K. Denki, Denki Kagaku Oyobi Kogyo Butsuri Kagaku 49 (1) (1981) 19–21.
[3] J. Kutscher, A. Schneider, Z. Anorg. Allg. Chem. 386 (1971) 38.
[4] J.A. Baglio, C.W. Struck, in: Proceedings of 10th International IUPAC Conference on High Temperature Materials Chemistry, Julich, Germany, 2000.
[5] R. Takagi, L. Rycerz, M. Gaune-Escard, in: Electrochemical Society Proceedings of the Ninth International Symposium on Molten Salts, Vol. 94, No. 13, 1994, pp. 99–107.

[6] R. Takagi, L. Rycerz, M. Gaune-Escard, Denki Kagaku 62 (3) (1994) 240–245.
[7] A.K. Adya, R. Takagi, M. Sakurai, M. Gaune-Escard, in: Electrochemical Society Proceedings of the 11th International Symposium on Molten Salts, Vol. 98, No. 11, 1998, pp. 499–512.
[8] J.W. Hastie, D.W. Bonnell, High Temp. Sci. 19 (1985) 275.
[9] K.E. Spear, T.M. Besmann, E.C. Beahm, MRS Bull. 24 (1999) 37, and references therein.
[10] M.W. Chase Jr., JANAF Thermochemical Tables, 4th Edition, American Chemical Society and American Institute of Physics for the National Institute of Standards and Technology, New York, 1988.
[11] C.W. Struck, J.A. Baglio, High Temp. Sci. 31 (1991) 209–237.
[12] D.L. Hildenbrand, K.H. Lau, Private communication.
[13] K. Hilpert, U. Niemann, Thermochem. Acta 299 (1997) 49, and references therein.